Supporting Information

Sum Frequency Generation of Interfacial Lipid Monolayers Shows Polarization Dependence on Experimental Geometries

Bolin Li,[†] Xu Li,[†] Yong-Hao Ma,[†] Xiaofeng Han,[†] Fu-Gen Wu,[†] Zhirui Guo[‡], Zhan Chen[§], and Xiaolin Lu,*[,†]

[†]*State Key Laboratory of Bioelectronics, School of Biological Science and Medical Engineering, Southeast University, Nanjing 210096, China*

[‡]*Department of Geriatrics, the Second Affiliated Hospital of Nanjing Medical University, Nanjing 210029, P. R. China*

[§]*Department of Chemistry, University of Michigan, 930 North University Avenue, Ann Arbor, Michigan 48109, United States*

Corresponding Author

Xiaolin Lu

E-mail: lxl@seu.edu.cn.

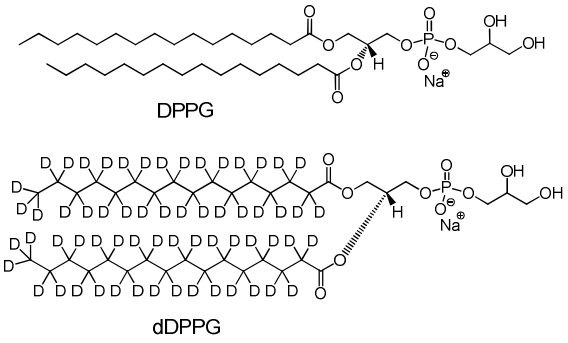

Figure S1. Molecular formulas of the DPPG and dDPPG employed in this study.

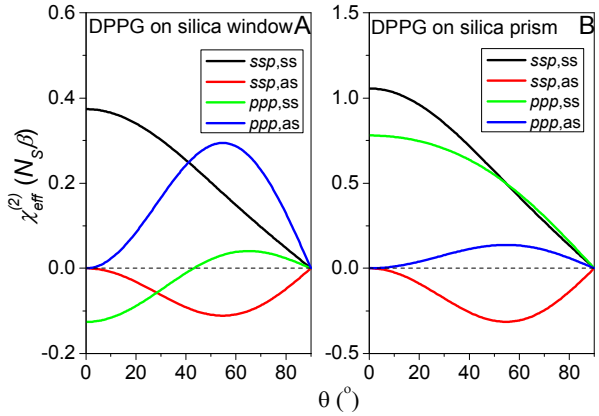

Figure S2. Dependence of $\chi_{eff}^{(2)}$ on the methyl tilt angle (θ) (assuming a δ-distribution) for methyl "ss" and "as" modes in *ssp* and *ppp* spectra collected using the silica window (A) and silica prism (B) geometries. The dashed lines are just used for guiding eyes.

For the interfacial Fresnel coefficient calculation, only the 1–0 interface should be considered for the silica window geometry, as shown in Figure S3A. Numbers 1 and 0 represent the air and silica media, respectively. For the two input beams (for simplification, only one input beam is depicted here) focusing at the 1–0 interface, φ_1 stands for the incident angle of these two input beams at the 1–0 interface versus the surface normal ($\varphi_1 = 65°$ for visible and $\varphi_1 = 54°$ for infrared in this study). Therefore, the transmitted angle φ_0 of these two beams can be expressed as eqn S1.

$$\varphi_0 = \arcsin\left(\frac{n_1}{n_0}\sin\varphi_1\right) \qquad \text{(S1)}$$

Here n_i (i = 1 or 0) is the refractive index of the corresponding medium, which are listed in table S1. Assuming the output angle of the SFG signal beam at the 1–0 interface is φ_{1su}, the φ_{1su} can be written as eqn S2:

$$\varphi_{1su} = \arcsin\left(\frac{\lambda_{su}}{n_{1su}}\times\left(\frac{n_{1vi}\times\sin\varphi_{1vi}}{\lambda_{vi}}+\frac{n_{1in}\times\sin\varphi_{1in}}{\lambda_{in}}\right)\right) \qquad \text{(S2)}$$

Using these input and output angles, we can calculate the interfacial Fresnel coefficients of a DPPG monolayer on a silica window. For the 1–0 interface, the following eqns S3–S5 can account for the Fresnel coefficients for the interfacial layer at different directions (*x*, *y*, or *z*).[1] These equations are applicable to both input and output beams. So here no subscripts are marked.

$$L_{xx}(\omega_i) = \frac{2n_1\cos\varphi_0}{n_1\cos\varphi_0 + n_0\cos\varphi_1} \qquad \text{(S3)}$$

$$L_{yy}(\omega_i) = \frac{2n_1\cos\varphi_1}{n_1\cos\varphi_1 + n_0\cos\varphi_0} \qquad \text{(S4)}$$

$$L_{zz}(\omega_i) = \frac{2n_0\cos\varphi_1}{n_1\cos\varphi_0 + n_0\cos\varphi_1}\cdot\frac{n_1^2}{n'^2} \qquad \text{(S5)}$$

Here n' represents the refractive index of the interfacial layer (See Table S1).[1,2] the average refractive index of the silica and air were used for the n'.[3] L_{ii} ($i = x$, y, or z) is the interfacial Fresnel coefficient for input and output beams.

Together with the above equations, the overall interfacial Fresnel coefficients for the silica window geometry can be calculated using eqns S6-S10 for *ssp* and *ppp* polarization combinations:

$$F_{ssp,yyz} = L_{yy}(\omega_{su})L_{yy}(\omega_{vi})L_{zz}(\omega_{in})\sin\varphi_{1,in} \qquad \text{(S6)}$$

$$F_{ppp,xxz} = -L_{xx}(\omega_{su})cos\varphi_{1,su}L_{xx}(\omega_{vi})cos\varphi_{1,vi}L_{zz}(\omega_{in})sin\varphi_{1,in} \quad \text{(S7)}$$

$$F_{ppp,xzx} = -L_{xx}(\omega_{su})cos\varphi_{1,su}L_{zz}(\omega_{vi})\sin\varphi_{1,vi}L_{xx}(\omega_{in})\cos\varphi_{1,in} \quad \text{(S8)}$$

$$F_{ppp,zxx} = L_{zz}(\omega_{su})\sin\varphi_{1,su}L_{xx}(\omega_{vi})\cos\varphi_{1,vi}L_{xx}(\omega_{in})\cos\varphi_{1,in} \quad \text{(S9)}$$

$$F_{ppp,zxx} = L_{zz}(\omega_{su})\sin\varphi_{1,su}L_{zz}(\omega_{vi})\sin\varphi_{1,vi}L_{zz}(\omega_{in})\sin\varphi_{1,in} \quad \text{(S10)}$$

For the interfacial Fresnel coefficient calculation of the silica prism geometry shown in Figure S3B, three interfaces should be considered. Medium 0 represents the prism; media 1, 2, and 3 represent the air. For simplification, only one input beam was shown. For the two input beams, σ_0 is the incident angle at the 1–0 interface ($\sigma_1 = 25°$ for visible and $\sigma_1 = 36°$ for infrared versus the surface normal in this research). So the transmitted angle σ_0 of the two beams can be acquired from eqn S11:

$$\sigma_0 = \arcsin\left(\frac{n_1}{n_0}\sin\sigma_1\right) \quad \text{(S11)}$$

Supposing the incident angle of the input beam is φ_0 at the 0–2 interface, it can thus be calculated as $\varphi_0 = \pi/2 - \sigma_1$. The SFG signal was generated at the interfacial layer and then reflected back into the medium 0 again. The reflected SFG signal beam subsequently passed through the 0–3 interface, and was finally detected by the monochromator/PMT. Assuming that the reflected angle of the SFG signal beam at the 0–2 interface is φ_{0su}, and thus the incident angle of the SFG signal beam at the 0–3 interface is $\sigma_{0su} = \varphi_{0su} - \pi/4$. So the output angle of the SFG signal beam at the 0–3 interface can be expressed as eqn S12:

$$\sigma_{3su} = \arcsin\left(\frac{n_0}{n_3}\sin\sigma_{0su}\right) \quad \text{(S12)}$$

Using these angles, we can calculate the interfacial Fresnel coefficients of a DPPG lipid monolayer for the silica prism geometry. At the 1–0 interface, eqns S13–S16 can account for the two input beams transmitting from air into the silica prism:

$$t_{10vi}^{s} = \frac{2n_{1vi}\cos\sigma_{1vi}}{n_{1vi}\cos\sigma_{1vi} + n_{0vi}\cos\sigma_{0vi}} \quad \text{(S13)}$$

$$t_{10vi}^{p} = \frac{2n_{1vi}\cos\sigma_{1vi}}{n_{0in}\cos\sigma_{1vi} + n_{1vi}\cos\sigma_{0vi}} \quad \text{(S14)}$$

$$t_{10in}^{s} = \frac{2n_{1in}\cos\sigma_{1in}}{n_{1in}\cos\sigma_{1in} + n_{0in}\cos\sigma_{0in}} \quad \text{(S15)}$$

$$t_{10in}^{p} = \frac{2n_{1in}\cos\sigma_{1in}}{n_{0in}\cos\sigma_{1in} + n_{1vi}\cos\sigma_{0in}} \quad \text{(S16)}$$

At the 0–2 interface, the Fresnel coefficients for the input and output beams with respect to the interfacial layer can also be expressed as eqns S3–S5. And then at the 0–3 interface, eqns S17 and S18 can account for the output SFG signal beam transmitting from the silica into air and finally being detected:

$$t_{03su}^{s} = \frac{2n_{0su}\cos\sigma_{0su}}{n_{0su}\cos\sigma_{0su} + n_{3su}\cos\sigma_{3su}} \quad \text{(S17)}$$

$$t_{03su}^{p} = \frac{2n_{0su}\cos\sigma_{0su}}{n_{3su}\cos\sigma_{0su} + n_{0su}\cos\sigma_{3su}} \quad \text{(S18)}$$

Finally, the overall interfacial Fresnel coefficients can be acquired for the silica prism geometry:

$$F_{ssp,yyz} = t_{03su}^{s} L_{yy}(\omega_{su}) t_{10vi}^{s} L_{yy}(\omega_{vi}) t_{10in}^{p} L_{zz}(\omega_{in}) \sin\varphi_{0,in} \quad \text{(S19)}$$

$$F_{ppp,xxz} = -t_{03su}^{p} L_{xx}(\omega_{su}) \cos\varphi_{0,su} t_{10vi}^{p} L_{xx}(\omega_{vi}) \cos\varphi_{0,vi} t_{10in}^{p} L_{zz}(\omega_{in}) \sin\varphi_{0,in} \quad \text{(S20)}$$

$$F_{ppp,xzx} = -t_{03su}^{p} L_{xx}(\omega_{su}) \cos\varphi_{0,su} t_{10vi}^{p} L_{zz}(\omega_{vi}) \sin\varphi_{0,vi} t_{10in}^{p} L_{xx}(\omega_{in}) \cos\varphi_{0,in} \quad \text{(S21)}$$

$$F_{ppp,zxx} = t_{03su}^{p} L_{zz}(\omega_{su}) \sin\varphi_{0,su} t_{10vi}^{p} L_{xx}(\omega_{vi}) \cos\varphi_{0,vi} t_{10in}^{p} L_{xx}(\omega_{in}) \cos\varphi_{0,in} \quad \text{(S22)}$$

$$F_{ppp,zxx} = t_{03su}^{p} L_{zz}(\omega_{su}) \sin\varphi_{0,su} t_{10vi}^{p} L_{zz}(\omega_{vi}) \sin\varphi_{0,vi} t_{10in}^{p} L_{zz}(\omega_{in}) \sin\varphi_{0,in} \quad \text{(S23)}$$

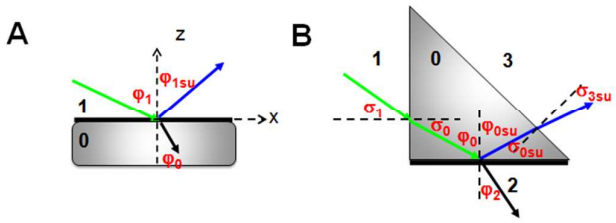

Figure S3. Propagation of the light beam was also plotted for these two geometries (A and B, for simplification, only one input beam was shown).

Table S1. Refractive index of the corresponding medium

Refractive index (n_i)	Visible beam	Infrared beam	Sum frequency beam
Silica (n_0)[4]	1.46	1.41	1.46
Air (n_1)[4]	1	1	1
Silica/lipid/air interfacial layer (n')[3]	1.23	1.21	1.23

n': the average refractive index of the silica and the air

For the calculation of the molecular hyperpolarizability tensor component, a bond additive approach can be employed.[5] So we have:

$$\beta_{aac} = \beta_{bbc} = \frac{4+5\rho}{9} \cdot a_0 \cdot \frac{1}{\omega - \omega_s + i\Gamma_s}$$

$$\beta_{ccc} = \frac{1+8\rho}{9} \cdot a_0 \cdot \frac{1}{\omega - \omega_s + i\Gamma_s}$$

$$\beta_{aca} = \beta_{bcb} = 4\frac{1-\rho}{9} \cdot a_0 \cdot \frac{1}{\omega - \omega_{as} + i\Gamma_{as}}$$

Here a_0 is related to the product of the infrared transition moment and Raman polarizability tensors, and ρ is the ratio of the Raman polarizability tensor components perpendicular and parallel for the single C-H bond.[6] Based on previous studies, we have ρ = 0.14.[7,8] so r = $\beta_{aac,ss}/\beta_{ccc,ss}$ = 2.2, which is in the reasonable range from 1.5 to 4 for the methyl group as reported by literatures.[9–15]

According to earlier study.[16] we have:

$$\frac{\beta_{aca,as}}{\beta_{ccc,ss}} = \frac{\beta_{caa,as}}{\beta_{ccc,ss}} = \frac{\omega_{ss}}{\omega_{as}} \cdot \frac{4(1-\rho)}{1+8\rho} \cdot \frac{G_E}{G_{A1}}$$

And $\frac{G_E}{G_{A1}} = \frac{40}{37}$

So the $\beta_{aca,as}/\beta_{ccc,ss}$ is 1.7.

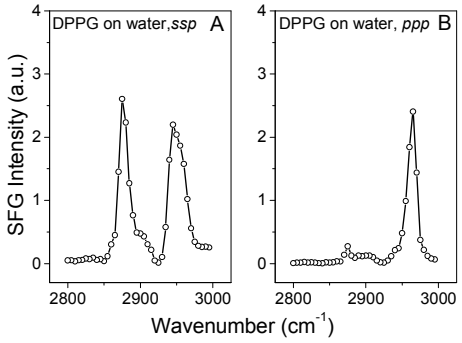

Figure S4. SFG *ssp* (A) and *ppp* (B) spectra of a DPPG monolayer on water.

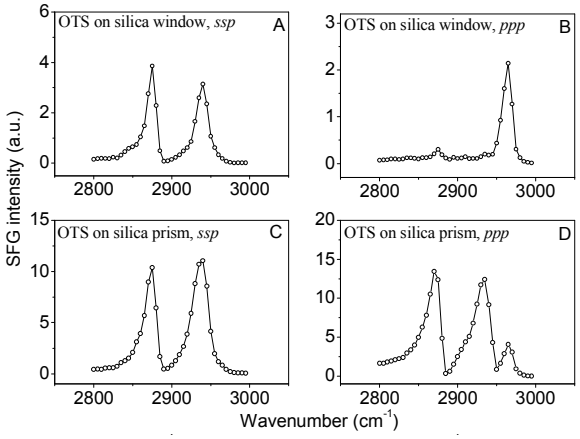

Figure S5. SFG *ssp* and *ppp* spectra of the self-assembled octadecyltrichlorosilane (OTS) monolayer on silica window (A and B) and silica prism (C and D).

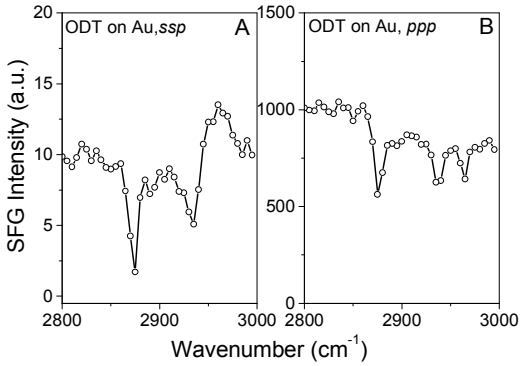

Figure S6. SFG *ssp* (A) and *ppp* (B) spectra of an Octadecanethiol (ODT) monolayer on Au.

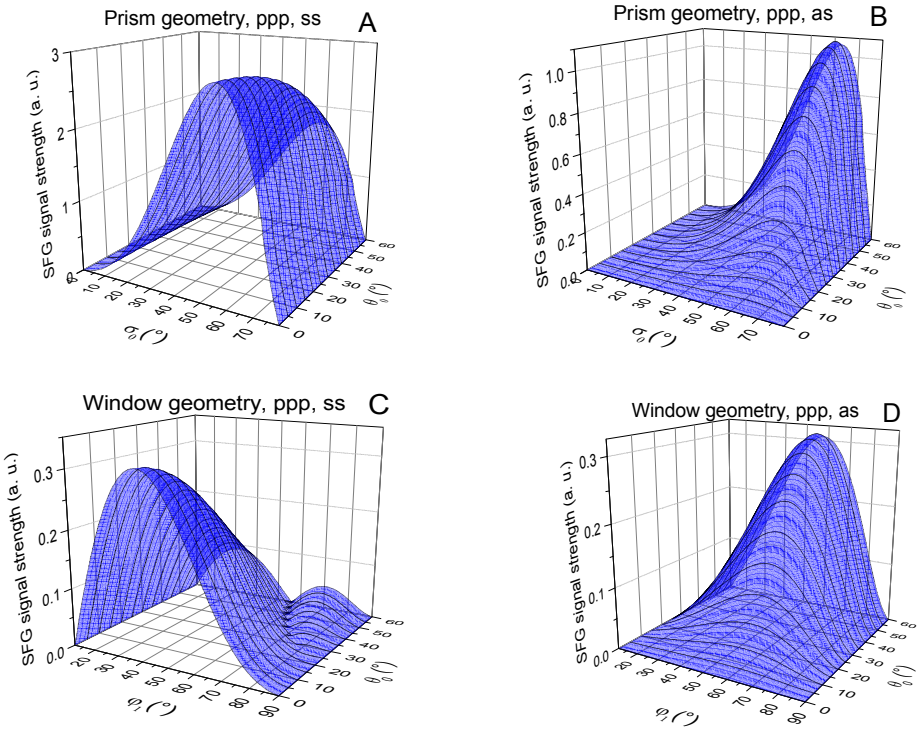

Figure S7. SFG *ppp* signal strength dependence on the visible bean input angle (σ_0 or φ_1) and average tilt angle θ_0 of CH_3 group for both the silica prism (A and B) and silica window (C and D) geometries. φ_1 and σ_0 represent the visible beam input angles for the silica window and silica prism geometries, respectively. The angle difference between visible and infrared beams is fixed at 11° for both geometries.

References

(1) Zhuang, X. W.; Miranda, P. B.; Kim, D.; Shen, Y. R. Mapping Molecular Orientation and Conformation at Interfaces by Surface Nonlinear Optics. *Phys. Rev. B* **1999**, *59*, 12632–12640.

(2) Simpson, G. J.; Dailey, C. A.; Plocinik, R. M.; Moad, A. J.; Polizzi, M. A.; Everly, R. M. Direct Determination of Effective Interfacial Optical Constants by Nonlinear Optical Null Ellipsometry of Chiral Films. *Anal. Chem*. **2005**, *77*, 215–224.

(3) Simpson, G. J.; Dailey, C. A.; Plocinik, R. M.; Moad, A. J.; Polizzi, M. A.; Everly, R. M. Direct Determination of Effective Interfacial Optical Constants by Nonlinear Optical Null Ellipsometry of Chiral Films. *Anal. Chem*. **2005**, *77*, 215–224.

(4) http://refractiveindex.info/?shelf=main&book=SiO2&page=Malitson

(5) Pászti, Z.; Wang, J.; Clarke, M. L.; Chen, Z. Sum Frequency Generation Vibrational Spectroscopy Studies of Protein Adsorption on Oxide-Covered Ti Surfaces. *J. Phys. Chem. B* **2004**, *108*, 7779–7787.

(6) Hirose, C.; Akamatsu, N.; Domen, K. Formulas for the Analysis of Surface Sum-Frequency Generation Spectrum by CH Stretching Modes of Methyl and Methylene Groups. *J. Chem. Phys*. **1992**, *96*, 997–1004.

(7) Oh-e, M.; Lvovsky, A. I.; Wei, X.; Shen, Y. R. Sum-Frequency Generation (SFG) Vibrational Spectroscopy of Side Alkyl Chain Structures of Polyimide Surfaces. *J. Chem. Phys.* **2000**, *113*, 8827–8832.

(8) Hirose, C.; Yamamoto, H.; Akamatsu, N.; Domen, K. Orientation Analysis by Simulation

of Vibrational Sum Frequency Generation Spectrum: CH Stretching Bands of the Methyl Group. *J. Phys. Chem*. **1993**, *97*, 10064–10069.

(9) Zhuang, X. W.; Miranda, P. B.; Kim, D.; Shen, Y. R. Mapping Molecular Orientation and Conformation at Interfaces by Surface Nonlinear Optics. *Phys. Rev. B* **1999**, *59*, 12632–12640.

(10) Hirose, C.; Akamatsu, N.; Domen, K. Formulas for the Analysis of Surface Sum-Frequency Generation Spectrum by CH Stretching Modes of Methyl and Methylene Groups. *J. Chem. Phys*. **1992**, *96*, 997–1004.

(11) Pászti, Z.; Wang, J.; Clarke, M. L.; Chen, Z. Sum Frequency Generation Vibrational Spectroscopy Studies of Protein Adsorption on Oxide-Covered Ti Surfaces. *J. Phys. Chem. B* **2004**, *108*, 7779–7787.

(12) Bell, G. R.; Li, Z. X.; Bain, C. D.; Fischer, P.; Duffy, D. C. Monolayers of Hexadecyltrimethylammonium *p*-Tosylate at the Air−Water Interface. 1. Sum-Frequency Spectroscopy. *J. Phys. Chem. B* **1998**, *102*, 9461–9472.

(13) Guyot-Sionnest, P.; Hunt, J. H.; Shen, Y. R. Sum-Frequency Vibrational Spectroscopy of a Langmuir Film: Study of Molecular Orientation of a Two-Dimensional System. *Phys. Rev. Lett*. **1987**, *59*, 1597–1600.

(14) Wolfram, K.; Laubereau, A. Vibrational Sum-Frequency Spectroscopy of an Adsorbed Monolayer of Hexadecanol on Water. Destructive Interference of Adjacent Lines. *Chem. Phys. Lett.* **1994**, *228*, 83–88.

(15) Wang, H. F.; Gan, W.; Lu, R.; Rao, Y.; Wu, B. H. Quantitative Spectral and Orientational

Analysis in Surface Sum Frequency Generation Vibrational Spectroscopy (SFG-VS). *Int. Rev. Phys. Chem*. **2005**, *24*, 191–256.

(16) Wu, H.; Zhang, W. K.; Gan, W.; Cui, Z. F.; Wang, H. F. An Empirical Approach to the Bond Additivity Model in Quantitative Interpretation of Sum Frequency Generation Vibrational Spectra. *J. Chem. Phys*. **2006**, *125*, 133203.